HHS Public Access

Author manuscript

Dev Biol. Author manuscript; available in PMC 2018 February 27.

Published in final edited form as:

Dev Biol. 2017 September 01; 429(1): 240–248. doi:10.1016/j.ydbio.2017.06.022.

Distinct *cis* elements in the 3′ UTR of the *C. elegans cebp-1* mRNA mediate its regulation in neuronal development

Panid Sharifnia[a], **Kyung Won Kim**[a], **Zilu Wu**[b], and **Yishi Jin**[a,b,*]

[a]Section of Neurobiology, Division of Biological Sciences, University of California San Diego, La Jolla, CA 92093, USA

[b]Howard Hughes Medical Institute, USA

Abstract

The 3′ untranslated regions (3′ UTRs) of mRNAs mediate post-transcriptional regulation of genes in many biological processes. *Cis* elements in 3′ UTRs can interact with RNA-binding factors in sequence-specific or structure-dependent manners, enabling regulation of mRNA stability, translation, and localization. *Caenorhabditis elegans* CEBP-1 is a conserved transcription factor of the C/EBP family, and functions in diverse contexts, from neuronal development and axon regeneration to organismal growth. Previous studies revealed that the levels of *cebp-1* mRNA in neurons depend on its 3′ UTR and are also negatively regulated by the E3 ubiquitin ligase RPM-1. Here, by systematically dissecting *cebp-1*'s 3′ UTR, we test the roles of specific *cis* elements in *cebp-1* expression and function in neurons. We present evidence for a putative stem-loop in the *cebp-1* 3′ UTR that contributes to basal expression levels of mRNA and to negative regulation by *rpm-1*. Mutant animals lacking the endogenous *cebp-1* 3′ UTR showed a noticeable increased expression of *cebp-1* mRNA and enhanced the neuronal developmental phenotypes of *rpm-1* mutants. Our data reveal multiple *cis* elements within *cebp-1*'s 3′ UTR that help to optimize CEBP-1 expression levels in neuronal development.

Keywords

rpm-1; Mechanosensory neurons; Axon regeneration; mRNA secondary structure; Stem-loop; Translation regulation; mRNA stability

1. Introduction

Numerous mechanisms involving post-transcriptional regulation of mRNA contribute to temporal and spatial control of neuronal responses to a variety of stimuli (Holt and Schuman, 2013). For example, local translation of mRNA in presynaptic terminals is induced by neuronal activity, and in turn regulates synaptic plasticity in *Aplysia* (Martin et al., 1997). Alternative splicing is a key step in the production of specific isoforms of the synaptic membrane protein neurexin, enabling different receptor interactions in mammalian hippocampal synapses (Traunmuller et al., 2016). The importance of understanding mRNA

*Corresponding author at: Section of Neurobiology, Division of Biological Sciences, University of California San Diego, La Jolla, CA 92093, USA. yijin@ucsd.edu (Y. Jin).

regulation in the nervous system is cemented by the notion that several neurological diseases are linked to RNA-binding proteins, such as TDP43 and FMRP (Ibrahim et al., 2012; Liu-Yesucevitz et al., 2011).

Many studies have shown that *cis* elements in 5′ or 3′ untranslated regions (UTRs) of mRNA regulate mRNA stability, splicing, translation and localization (Mignone et al., 2002). microRNA mediated regulation is prevalent in temporal and spatial control of mRNA translation and stability, and generally acts through matching sequences in the 3′ UTR (Fabian et al., 2010). Other types of *cis* elements can function in a sequence- or structure-dependent manner. For example, the "zipcode" in the 3′ UTR of β-actin consists of ~ 50 nucleotides that form a stem-loop structure, which is recognized by the Zipcode Binding Proteins (ZBPs) to regulate the localization and translation of β-actin mRNA (Kislauskis et al., 1994; Ross et al., 1997). In yeast, subcellular localization of ASH1 mRNA also depends on a stem-loop structure in its 3′ UTR (Chartrand et al., 1999; Gonzalez et al., 1999). In bacteria, stem-loops in the 3′ terminal ends of *puf* mRNA regulate its stability (Belasco and Chen, 1988; Chen et al., 1988). In *Aplysia* neurons, unique *cis* elements in the 5′ or 3′ UTR of mRNAs of the neuropeptide sensorin mediate differential control of its mRNA localization and translation (Meer et al., 2012). A long 3′ UTR in the importin β mRNA is necessary for axonal retrograde signaling in response to injury in mice (Perry et al., 2012).

In *C. elegans, cebp-1* encodes a conserved transcription factor of the C/EBP family, and is a key downstream target of the DLK-1 and p38 MAP kinase cascade (Yan et al., 2009). This kinase cascade plays important roles in neuronal development and stress response, and is under the negative control of the E3 ubiquitin ligase RPM-1 (Nakata et al., 2005). We previously showed that regulation of mRNA stability and translation of *cebp-1* involves its 3′ UTR (Yan et al., 2009). Here, we address the function of specific *cis* regulatory elements in the *cebp-1* 3′ UTR. We show that multiple *cis* elements in *cebp-1* 3′ UTR contribute to its expression level in neurons. Our data suggest that an RNA secondary structure based mechanism regulates the efficiency of translation of *cebp-1* mRNA, dependent on the activity of RPM-1.

2. Results

2.1. Identification of cis elements in the 3′ UTR of cebp-1

To gain clues for *cis* elements that regulate *cebp-1* mRNA, we compared the 3′ UTR sequence of *C. elegans cebp-1* to those of *C. brenneri cebp-1* and mouse C/EBPδ and identified several regions with conserved sequences (Fig. S1A). miRNA prediction programs also suggest possible seed sequences within nucleotides 79–98 (seed element A) of *cebp-1* 3′ UTR, for example, CATTCC, matching those for *mir-1* (Materials and Methods). To assess the roles of these predicted elements in regulating *cebp-1* transcripts, we generated a series of deletions of the 3′ UTR and placed these downstream of a destabilized GFP reporter (DsGFP), a sensitive readout for dynamic expression (Frand et al., 2005; Li et al., 1998) (Fig. S1B). As *cebp-1* is expressed in many tissues (Kim et al., 2016), to address 3′ UTR-mediated regulation specifically in the nervous system, we used the pan-neuronal *rgef-1* promoter to drive transgene expression. We initially analyzed transgenic lines generated as high-copy extra-chromosomal arrays. While we observed that removal of three

elements affected DsGFP expression by visual inspection of fluorescence intensity (Fig. S1C), we also observed highly variable expression among different lines generated with the same construct, likely due to the variable nature of extra-chromosomal arrays.

To precisely compare expression levels involving specific sequence elements in *cebp-1* 3′ UTR, we next generated stably integrated single-copy transgenes on chromosome II using MosSCI methodology (Frokjaer-Jensen et al., 2008). We used GFP as a reporter to facilitate visual assessment in this series of reporters (Fig. 1A). We quantitatively measured GFP fluorescent intensity in the nerve ring of animals at the 4th larval stage (L4) to discern changes in transgene expression. As a control for 3′ UTR specificity, we examined a similar reporter with the 3′ UTR of *unc-54*, which is commonly used in *C. elegans* transgenic expression (Fire et al., 1990). In wild type animals, deletion of the predicted microRNA seed element A did not affect GFP expression, compared to the full 3′ UTR reporter (Fig. 1C). Deletion of *cis* element D caused increased GFP expression (Fig. 1C). Removal of *cis* element E, which consists of stretches of repetitive A/Ts near the 3′ end of 3′ UTR, resulted in the largest increase in GFP intensity (Fig. 1C). The latter effect was not observed from the multi-copy transgenic lines (Fig. S1C), likely due to variable baseline expression of those high-copy number transgenes.

With the integrated single-copy reporters, we were able to quantitatively measure steady-state mRNA levels of GFP using qRT-PCR (Materials and Methods). The mRNA levels of GFP from the transgene with the full length *cebp-1* 3′ UTR were significantly lower than those with the transgene with the *unc-54* 3′ UTR. Interestingly, even though transgenes in which element D or E was deleted displayed higher levels of GFP fluorescence compared to the full-length 3′ UTR reporter, we observed no significant changes in GFP mRNA abundance by qRT-PCR (Fig. 1D). As these transgenes express GFP in the same set of neurons, these results suggest that the elements D and E individually may not directly affect mRNA stability, and that multiple elements in *cebp-1*'s 3′ UTR may regulate mRNA stability and translation in the nervous system.

2.2. Function of cis element D may involve a putative stem-loop structure

Secondary RNA structures regulate mRNA stability and translation (Wan et al., 2011). We therefore searched for possible secondary RNA structures in the *cebp-1* 3′ UTR, using the algorithms RNApromo (Rabani et al., 2008) and RNA fold (Hofacker et al., 1994; McCaskill, 1990; Zuker and Stiegler, 1981), both of which predicted similar stem loop structures within element D (Fig. S2A). To test this prediction we generated single-copy expression transgenes in which we deleted portions of element D (Fig. 2A, labeled as ΔD1 and ΔD2). Such deletions would likely disrupt the predicted RNA structure (Fig. S2B). Removal of element D2, but not D1, increased GFP fluorescence intensity, compared to the reporters for full-length 3′ UTR or ΔD (Fig. 2C). To further test if the predicted stem-loop structure was important for *cebp-1*'s 3′ UTR transgene expression, we mutated nucleotides ACTGG within the predicted stem to TTAAT (ΔD3 in Figs. 2A, S2C). This mutant construct showed up-regulation of GFP, similar to the ΔD2 transgene (Fig. 2B,C). Unlike other well-known hairpins (Kislauskis et al., 1994; Chartrand et al., 1999), the predicted hairpin stem length in element D of *cebp-1* 3′ UTR is relatively short (labeled stem loop #2 in Fig. S2A).

To test if this putative stem-loop could function independent of nucleotide sequence identity, we constructed a reporter that reversed the bases of the stem but retained the predicted stem-loop structure (Dsr in Fig. S2D). We found that GFP intensity from the Dsr transgene was similar to that of the full length 3′ UTR (Fig. 2C), supporting a conclusion that element D may form a secondary stem-loop structure.

We next assessed if changes of GFP fluorescence from the 3′ UTR transgenes with mutant *cis* element D affected mRNA stability. By qRT-PCR analysis, we found no statistically significant difference in GFP mRNA levels among animals expressing distinct *cebp-1* 3′ UTR deletion transgenes or mutated stem loop transgenes, compared to the full-length reporter (Fig. 2D). We also cultured animals in the presence of α-amanitin, an inhibitor of transcription, and found that levels of GFP mRNA from these transgenes remained similar to those of full-length *cebp-1* 3′ UTR controls (Fig. S3). Together, these findings suggest that *cis* element D may regulate the translation of mRNA via a stem-loop based mechanism.

2.3. rpm-1 negatively regulates cebp-1 3′ UTR transgene expression through two separate cis elements

The E3 ubiquitin ligase *rpm-1* negatively regulates the DLK-1 MAP kinase cascade, acting upstream of *cebp-1* (Yan et al., 2009). Loss of *rpm-1* function causes an increase in *cebp-1* mRNA levels. We next examined which of the *cis* elements in *cebp-1* 3′ UTR were necessary for *rpm-1*-dependent regulation. We generated strains expressing each single-copy transgene of *cebp-1* 3′ UTR in *rpm-1(lf)* mutants, and compared GFP fluorescence intensity from transgenic animals relative to those in the wild type background (Materials and Methods). Consistent with our previous findings (Yan et al., 2009), GFP intensity from the *cebp-1* full length 3′ UTR reporter showed significant increase in *rpm-1(lf)*, compared to that in wild type animals (Fig. 3A,B). Moreover, GFP mRNA abundance, measured by qRT-PCR, from the *cebp-1* full length 3′ UTR transgene, but not that from the transgene reporter with *unc-54* 3′ UTR, showed a similar increase in *rpm-1(lf)* (Fig. 3C).

Similar to the transgenic animals expressing reporters with the full-length 3′ UTR of *cebp-1*, the *cebp-1* 3′ UTR deletion transgenes with ΔA, ΔB or ΔE all showed increased GFP fluorescence in *rpm-1(lf)* (Fig. 3B). In contrast, 3′ UTR transgenes with ΔC or ΔD did not show detectable changes in *rpm-1(lf)*. Similar results were also observed using extra-chromosomal arrays, arguing against expression from these reporters being strongly dependent on insertion position in the genome (Fig. S1C). Moreover, quantitative comparisons of GFP mRNA levels showed no differences from the ΔC or ΔD transgene (Fig. 3C), suggesting that both elements may mediate the regulation of mRNA stability by *rpm-1*.

Since our data above support a role of RNA secondary structure in element D, we further examined if this structural element could be involved in *rpm-1* mediated regulation. Expression from the ΔD1 transgene showed dependency on *rpm-1*, similar to the full-length *cebp-1* 3′ UTR. In contrast, the ΔD2 transgene showed no change in fluorescence intensity, nor in mRNA levels, of GFP in *rpm-1(lf)*, compared to wild type (Fig. 3B,C). Interestingly, the ΔD2 transgene showed even higher levels of GFP expression, relative to all other transgenes. *rpm-1* may negatively regulate mRNA stability through element C, and mRNA translation through the putative stem-loop structure in element D.

Lastly, we wanted to investigate the role of the *cis* element D with single cell resolution. We expressed the Dendra fluorescent reporter with either full-length or ΔD2 *cebp-1* 3′ UTR, driven by the *mec-4* promoter for mechanosensory neurons, in multiple extra-chromosomal arrays (Materials and Methods). We analyzed fluorescence intensity in the somas of posterior lateral microtubule (PLM) neurons. In wild type backgrounds, average fluorescence intensity from ΔD2 transgene was similar to that from full-length 3′ UTR transgene. However, in *rpm-1(lf)* animals, ΔD2 transgenic reporters did not show any increase in fluorescence intensity, whereas fluorescence intensity from transgenes of full-length *cebp-1* 3′ UTR was increased, as expected (Fig. S4B), and consistent with the conclusion that element D plays a key role in regulating *cebp-1* mRNA depending on the type of neuron.

2.4. Deletion of 3′ UTR cis elements causes partial impairment of cebp-1 function in neuronal development and axon regeneration

A key question is whether the 3′ UTR *cis* elements are required for normal CEBP-1 function in vivo. To address this, we undertook functional rescue experiments of *cebp-1*'s function in PLM neuronal development and axon regeneration.

In wild type animals, the PLM axon extends from its cell body and terminates before the cell body of the anterior lateral microtubule (ALM) mechanosensory neuron, and also extends a branch to the ventral nerve cord to form synapses (synaptic branch) (Fig. 4A,B). In *rpm-1(lf)*, the PLM axon pattern is disrupted, with approximately 40% of animals displaying axon overextension and loss of synaptic branch (Fig. 4A,D). *cebp-1(0)* strongly suppresses this *rpm-1(lf)* developmental phenotype (Yan et al., 2009). To examine the impact of *cis* elements in *cebp-1* 3′ UTR on *cebp-1* function, we generated single-copy transgenes expressing full-length CEBP-1 protein tagged to GFP with different 3′ UTRs, driven by the pan-neuronal *rgef-1* promoter (Fig. 4C). In *cebp-1(0)* background, these transgenes did not affect PLM neuronal morphology (Fig. S5A,B). Expression of transgenes with full length 3′ UTR of *cebp-1* (*juSi127*) fully rescued the suppression of *rpm-1(lf)* by *cebp-1(0)* (Fig. 4D). However, the other transgenes, containing either *cebp-1* 3′ UTR ΔD2 (*juSi220)* or ΔE (*juSi222*), or the *unc-54* 3′ UTR (*juSi126*), failed to rescue (Fig. 4D). As PLM developmental phenotype in *rpm-1(lf)* is associated with an increase in *cebp-1* mRNA, we next measured *cebp-1* mRNA produced by these transgenes. Compared to the transgene with full *cebp-1* 3′ UTR, the other three transgenes all showed noticeable increase, with *juSi220* showing a statistically significant difference (Fig. 4E). These observations support a conclusion that *cis* elements within *cebp-1* 3′ UTR are critical for optimizing *cebp-1* activity in PLM neuronal development.

In adult *C. elegans*, laser axotomy to PLM axons triggers a robust regrowth response that is abrogated in *cebp-1(0)* mutants (Yan et al., 2009). We tested how the *cis* elements of *cebp-1* 3′ UTR might affect *cebp-1* function in PLM regeneration. We found that in *cebp-1(0)* animals, *cebp-1* expressed with its full 3′ UTR (*juSi127*) or with ΔD2 (*juSi220)* or ΔE deletion (*juSi222*) or with *unc-54* 3′ UTR rescued the failed axon regeneration phenotype to different degrees, with *juSi220* being the most efficient in rescuing regeneration defects of

cebp-1(0) (Fig. S5C, Supplementary Table 1). These data suggest that 3′ UTR mediated regulation of *cebp-1* activity is highly sensitive to biological contexts.

2.5. CRISPR deletion of the endogenous cebp-1 3′ UTR enhances neuronal defects in rpm-1(lf)

To directly address the effect of the *cis* elements on endogenous *cebp-1* function, we next used CRISPR-Cas9 genome editing technology to delete regions of the 3′ UTR from the *cebp-1* locus (Materials and Methods). Limited by the choice of effective sgRNAs, we obtained two deletion mutations, *ju1451* and *ju1452*, removing 462 and 454 bp, of the 3′ UTR, respectively (Fig. 5A). *cebp-1* mRNA levels in these two mutants showed a consistent trend of increased *cebp-1* mRNA compared to wild type, though this was not statistically significant (Fig. S6). Homozygous mutants for deletions in the 3′ UTR were viable and healthy, and did not significantly affect PLM axon development (Fig. 5B,D), nor had effects on nerve regeneration (Fig. 5E, Supplementary Table 2). However, in the *rpm-1(lf)* background, we found *ju1452* significantly enhanced the loss of PLM synaptic branch, compared to *rpm-1(lf)* alone (Fig. 5C). These results show that these *cis* elements within *cebp-1*'s 3′ UTR play functionally relevant roles in neuronal development in a manner depending on signaling strength.

3. Discussion

The C/EBP family of transcription factors has been studied for its many roles in different tissues, including the nervous system (Ramji and Foka, 2002). Mammalian genomes encode six members of this family, and *C. elegans* CEBP-1 is most similar to the mammalian C/EBPδ. We first identified *cebp-1* as necessary for axon regeneration, and this function is also reported for C/EBPδ in a mammalian axon regeneration model (Lopez de Heredia and Magoulas, 2013; Yan et al., 2009). The activity of *cebp-1* can be regulated at transcriptional and post-transcriptional levels (Kim et al., 2016; Yan et al., 2009). Here, we focused on post-transcriptional regulation involving the 3′ UTR of *cebp-1*, and our data reveal several *cis* elements contributing to context-dependent regulation of *cebp-1* function in the nervous system.

We have identified two *cis* elements D and E, in *cebp-1*'s 3′ UTR, that mediate its baseline expression. Our analysis on the expression levels of GFP reporters containing deletions and base-pair changes in element D further provides evidence that element D likely contains a stem-loop structure. Loss of *rpm-1* function results in increased stability of the full-length 3′ UTR reporter, but not the stability of the reporters with deletions in element D. These results suggest this putative stem-loop could be involved in the negative control of *cebp-1* during two different settings, one at baseline and another in response to *rpm-1* signaling. It is possible that this secondary structure serves as a scaffold for different *trans* factors to control *cebp-1* mRNA. Future efforts will be required to identify interacting proteins.

Our data show that elements C and D2 in *cebp-1* 3′ UTR are involved in the regulation of *cebp-1* by *rpm-1*. Since deletion of element C results in no difference in GFP fluorescence and mRNA levels in wild type animals, it suggests that this element is specifically important for mRNA stability regulation by *rpm-1*. However, with the removal of element D2, we

observed increased GFP fluorescence but not mRNA levels, suggesting that element D2 may affect translation. Thus, different *cis* elements in the 3′ UTR of *cebp-1* regulate the stability and translation of this transcription factor (Fig. 6). Interestingly a *cebp-1* homolog C/EBPδ is reported to be post-transcriptionally stabilized by a p38 MAPK cascade in response to ultra-violet radiation (Li et al., 2008), suggesting functional conservation of this regulation. Consistent with the moderate changes in expression levels from the 3′ UTR reporters, we find that these *cis* elements made modest contribution to *cebp-1* function in a context dependent manner. CEBP-1 protein expressed from transgenes with the *cebp-1 3′ UTR* deletion, or with a heterologous 3′ UTR of *unc-54*, did not rescue the touch neuron developmental defects in the *rpm-1(lf)*; *cebp-1(0)*. On the other hand, only CEBP-1 expressed from ΔD2 transgene fully rescued the axon regeneration defect. Previous observations have revealed that *cebp-1* acts in other dosage-dependent processes influencing larval development and axon regeneration (Kim et al., 2016, data not shown). These results indicate that the ability of the animal to tolerate changes in *cebp-1* levels is minimal, and that precise control over *cebp-1* levels may be accomplished by using multiple *cis* regulatory elements.

We note that *cebp-1* 3′ UTR mutations or single-copy transgenic animals in wild type background did not cause any defects even if the *cebp-1* mRNA levels are slightly increased. However, a previous study showed that overexpression of CEBP-1 using high-copy extrachromosomal transgenes in wild type background caused PLM axon termination defects (Yan et al., 2009). Such differences might reflect the dosage-sensitivity of PLM development to the CEBP-1 levels. Alternatively, the nature of transgenes might cause secondary effects on gene expression – for example, the copy number of the promoter or enhancer elements might induce competition of regulatory factors on endogenous genes in PLM development. As studies using single-copy transgene expression are made possible only recently, we foresee future work from *C. elegans* field would likely reveal mechanistic understanding.

In our experimental design, we used the heterologous pan-neuronal promoter, *rgef-1* to drive transgene expression. This allows precise assessment of the specific effects of individual *cis* elements in the 3′ UTR, but does not address whether *cis* elements function combinatorially with transcriptional regulation to affect CEBP-1 function. We addressed this caveat by generating deletions in the endogenous locus of *cebp-1* 3′ UTR. Due to technical constraints by sgRNA, the deletions were larger than those using single copy insertions. We found that these mutations in the 3′ UTR caused a trend of increased *cebp-1* mRNA. Although the deletions did not affect the development of the mechanosensory neurons or their regeneration, in conjunction with the *rpm-1(lf)* mutation, mutants lacking *cebp-1* 3′ UTR enhanced the loss of the PLM synaptic branch, suggesting *cebp-1*'s 3′ UTR is important for the formation of the synapse, similar to results observed using the single-copy transgenes. The difference in phenotype for axon regeneration and neural development suggests the dosage of *cebp-1* is more important during development than in the adult animal. With the deletion of its endogenous 3′ UTR the expression of *cebp-1* is sufficient for a regenerative response. However, during development *cebp-1* mRNA may be more precisely regulated through its 3′ UTR. Thus, when the 3′ UTR deletion mutations are combined with *rpm-1(lf)*, which already increases *cebp-1* mRNA, the combinatorial increase

in *cebp-1* mRNA disrupts neuronal development (Fig. 6). Since *cebp-1* has been found to function in other tissues as well as neurons, the *cebp-1* 3′ UTR may allow tissue and temporal specific regulation through different *cis* elements (Kim et al., 2016; McEwan et al., 2016). Overall, our findings on the *cebp-1* 3′ UTR are consistent with studies on the roles of post-transcriptional regulation mediated by 3′ UTR in other neuronal models. For example, removing regulatory elements in 3′ UTR of the Cam Kinase II reduce the amount of CamKII in postsynaptic density, and has modest effects on learning and memory behavior (Miller et al., 2002). Removal of the long 3′ UTR of importin β delays, but does not eliminate, retrograde signaling in axon injury response (Perry et al., 2012). Our data support the importance of *cis* elements in 3′ UTRs in post-transcriptional regulation in the nervous system. Future studies may reveal how other tissues employ similar mechanisms to regulate *cebp-1* activity.

Supplementary Material

Refer to Web version on PubMed Central for supplementary material.

Acknowledgments

We thank M. Andrusiak, S. Blazie, K. Noma, Y. Sun and A. D. Chisholm for comments on the manuscript, and our lab members for discussion. We thank J. Ewbank and N. Pujol and their lab members for their hospitality during P.S.'s study under her Chateaubriand Fellowship. P.S. was partly supported by NIH predoctoral training grant T32 GM008666; K.W.K by American Heart Association postdoctoral fellowship 13POST14800057. This work was supported by NIH R01 035546 and HHMI to Y.J.

Appendix A. Supporting information

Supplementary data associated with this article can be found in the online version at doi: 10.1016/j.ydbio.2017.06.022.

References

Belasco JG, Chen CY. Mechanism of puf mRNA degradation: the role of an intercistronic stem-loop structure. Gene. 1988; 72:109–117. [PubMed: 3243429]

Chartrand P, Meng XH, Singer RH, Long RM. Structural elements required for the localization of ASH1 mRNA and of a green fluorescent protein reporter particle in vivo. Curr Biol. 1999; 9:333–336. [PubMed: 10209102]

Chen CY, Beatty JT, Cohen SN, Belasco JG. An intercistronic stem-loop structure functions as an mRNA decay terminator necessary but insufficient for puf mRNA stability. Cell. 1988; 52:609–619. [PubMed: 2449287]

Fabian MR, Sonenberg N, Filipowicz W. Regulation of mRNA Translation and Stability for microRNAs. Annu Rev Biochem. 2010; 79:351–379. [PubMed: 20533884]

Fire A, Harrison SW, Dixon D. A modular set of *lacZ* fusion vectors for studying gene expression in *Caenorhabditis elegans*. Gene. 1990; 93:189–198. [PubMed: 2121610]

Frand AR, Russel S, Ruvkun G. Functional genomic analysis of *C. elegans* molting. PLoS Biol. 2005; 3:e312. [PubMed: 16122351]

Frokjaer-Jensen C, Davis MW, Hopkins CE, Newman BJ, Thummel JM, Olesen SP, Grunnet M, Jorgensen EM. Single-copy insertion of transgenes in *Caenorhabditis elegans*. Nat Genet. 2008; 40:1375–1383. [PubMed: 18953339]

Gonzalez I, Buonomo SB, Nasmyth K, von Ahsen U. ASH1 mRNA localization in yeast involves multiple secondary structural elements and Ash1 protein translation. Curr Biol. 1999; 9:337–340. [PubMed: 10209099]

Hofacker IL, Fontana W, Stadler PF, Bonhoeffer LS, Tacker M, Schuster P. Fast folding and comparison of RNA secondary structures. Mon Chem/Chem Mon. 1994; 125:167–188.

Holt CE, Schuman EM. The central dogma decentralized: new perspectives on RNA function and local translation in neurons. Neuron. 2013; 80:648–657. [PubMed: 24183017]

Ibrahim F, Nakaya T, Mourelatos Z. RNA dysregulation in diseases of motor neurons. Annu Rev Pathol. 2012; 7:323–352. [PubMed: 22035195]

Kim KW, Thakur N, Piggott CA, Omi S, Polanowska J, Jin Y, Pujol N. Coordinated inhibition of C/EBP by Tribbles in multiple tissues is essential for *Caenorhabditis elegans* development. BMC Biol. 2016; 14:104. [PubMed: 27927209]

Kislauskis EH, Zhu X, Singer RH. Sequences responsible for intracellular localization of beta-actin messenger RNA also affect cell phenotype. J Cell Biol. 1994; 127:441–451. [PubMed: 7929587]

Li B, Si J, DeWille JW. Ultraviolet radiation (UVR) activates p38 MAP kinase and induces post-transcriptional stabilization of the C/EBPdelta mRNA in G0 growth arrested mammary epithelial cells. J Cell Biochem. 2008; 103:1657–1669. [PubMed: 17902160]

Li X, Zhao X, Fang Y, Jiang X, Duong T, Fan C, Huang CC, Kain SR. Generation of destabilized green fluorescent protein as a transcription reporter. J Biol Chem. 1998; 273:34970–34975. [PubMed: 9857028]

Liu-Yesucevitz L, Bassell GJ, Gitler AD, Hart AC, Klann E, Richter JD, Warren ST, Wolozin B. Local RNA translation at the synapse and in disease. J Neurosci. 2011; 31:16086–16093. [PubMed: 22072660]

Lopez de Heredia L, Magoulas C. Lack of the transcription factor C/EBPdelta impairs the intrinsic capacity of peripheral neurons for regeneration. Exp Neurol. 2013; 239:148–157. [PubMed: 23099414]

Martin KC, Casadio A, Zhu H, Yaping E, Rose JC, Chen M, Bailey CH, Kandel ER. Synapse-specific, long-term facilitation of aplysia sensory to motor synapses: a function for local protein synthesis in memory storage. Cell. 1997; 91:927–938. [PubMed: 9428516]

McCaskill JS. The equilibrium partition function and base pair binding probabilities for RNA secondary structure. Biopolymers. 1990; 29:1105–1119. [PubMed: 1695107]

McEwan DL, Feinbaum RL, Stroustrup N, Haas W, Conery AL, Anselmo A, Sadreyev R, Ausubel FM. Tribbles ortholog NIPI-3 and bZIP transcription factor CEBP-1 regulate a *Caenorhabditis elegans* intestinal immune surveillance pathway. BMC Biol. 2016; 14:105. [PubMed: 27927200]

Meer EJ, Wang DO, Kim S, Barr I, Guo F, Martin KC. Identification of a cis-acting element that localizes mRNA to synapses. Proc Natl Acad Sci USA. 2012; 109:4639–4644. [PubMed: 22383561]

Mignone F, Gissi C, Liuni S, Pesole G. Untranslated regions of mRNAs. Genome Biol. 2002; 3 (reviews0004.1-0004.10).

Miller S, Yasuda M, Coats JK, Jones Y, Martone ME, Mayford M. Disruption of dendritic translation of CaMKIIα impairs stabilization of synaptic plasticity and memory consolidation. Neuron. 2002; 36:507–519. [PubMed: 12408852]

Nakata K, Abrams B, Grill B, Goncharov A, Huang X, Chisholm AD, Jin Y. Regulation of a DLK-1 and p38 MAP kinase pathway by the ubiquitin ligase RPM-1 is required for presynaptic development. Cell. 2005; 120:407–420. [PubMed: 15707898]

Perry RB, Doron-Mandel E, Iavnilovitch E, Rishal I, Dagan SY, Tsoory M, Coppola G, McDonald MK, Gomes C, Geschwind DH, et al. Subcellular knockout of importin beta1 perturbs axonal retrograde signaling. Neuron. 2012; 75:294–305. [PubMed: 22841314]

Rabani M, Kertesz M, Segal E. Computational prediction of RNA structural motifs involved in posttranscriptional regulatory processes. Proc Natl Acad Sci USA. 2008; 105:14885–14890. [PubMed: 18815376]

Ramji DP, Foka P. CCAAT/enhancer-binding proteins: structure, function and regulation. Biochem J. 2002; 365:561–575. [PubMed: 12006103]

Ross AF, Oleynikov Y, Kislauksi KH, Taneja K, Singer RH. Characterization of a β-actin mRNA zipcode-binding protein. Mol Cell Biol. 1997; 17:2158–2165. [PubMed: 9121465]

Schaefer AM, Hadwiger GD, Nonet ML. *rpm-1*, a conserved neuronal gene that regulates targeting and synaptogenesis in *C. elegans*. Neuron. 2000; 26:345–356. [PubMed: 10839354]

Traunmuller L, Gomez AM, Nguyen TM, Scheiffele P. Control of neuronal synapse specification by a highly dedicated alternative splicing program. Science. 2016; 352:982–986. [PubMed: 27174676]

Wan Y, Kertesz M, Spitale RC, Segal E, Chang HY. Understanding the transcriptome through RNA structure. Nat Rev Genet. 2011; 12:641–655. [PubMed: 21850044]

Yan D, Wu Z, Chisholm AD, Jin Y. The DLK-1 kinase promotes mRNA stability and local translation in *C. elegans* synapses and axon regeneration. Cell. 2009; 138:1005–1018. [PubMed: 19737525]

Zuker M, Stiegler P. Optimal computer folding of large RNA sequences using thermodynamics and auxiliary information. Nucleic Acids Res. 1981; 9:133–148. [PubMed: 6163133]

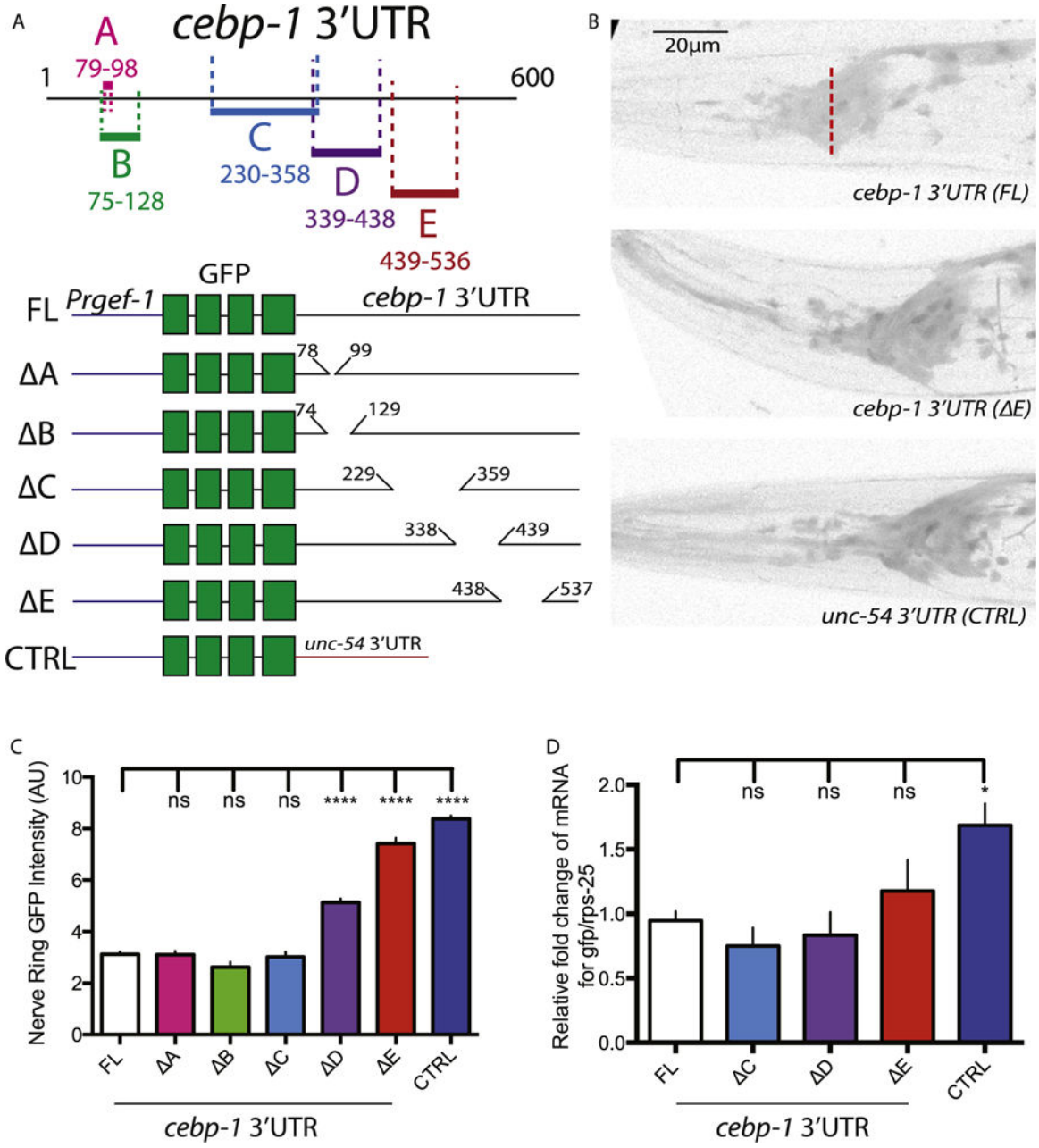

Fig. 1.

Identification of two *cis* elements in *cebp-1* 3′ UTR regulating reporter gene expression. A) Illustration of *cebp-1* 3′ UTR and transgene expression constructs. Top illustration shows full length 3′ UTR (1–600 nucleotides), with color labeling of *cis* elements examined in this study. Color scheme continues into other figures. *cebp-1* 3′ UTR reporter constructs GFP driven by Prgef-1 pan-neuronal promoter; and a control (CTRL) construct is with *unc-54* 3′ UTR. *Prgef-1* and GFP are not drawn to scale. All transgenes are inserted at *ttTi5606* on Chromosome II. FL represents full length *cebp-1* 3′ UTR, and Δ followed by a letter to denote the *cis* element deleted in the expression construct. B) Representative projection images of confocal Z-stack of GFP expression in the nerve ring for *cebp-1* 3′ UTR FL and

ΔE reporters, and the control 3′ UTR of *unc-54*. Dotted red line through *cebp-1* 3′ UTR shows example of line scan used for quantification of GFP using ImageJ. Scale bar, 20 μm. C) Quantification of GFP intensity in the nerve ring of L4 stage animals, n ≥ 10 for each genotype. AU: artificial unit; Error bars represent standard error of the mean (SEM). Statistics, One-way ANOVA with Tukey's post hoc tests; ns, not significant; **** $p < 0.0001$. D) qRT-PCR for GFP mRNA in L4 animals, ribosomal gene *rps-25* used as a reference. 3 biological replicates for each strain. Error bars, SEM; ns, not significant, * $p < 0.5$ (One-way ANOVA with Tukey's post hoc tests).

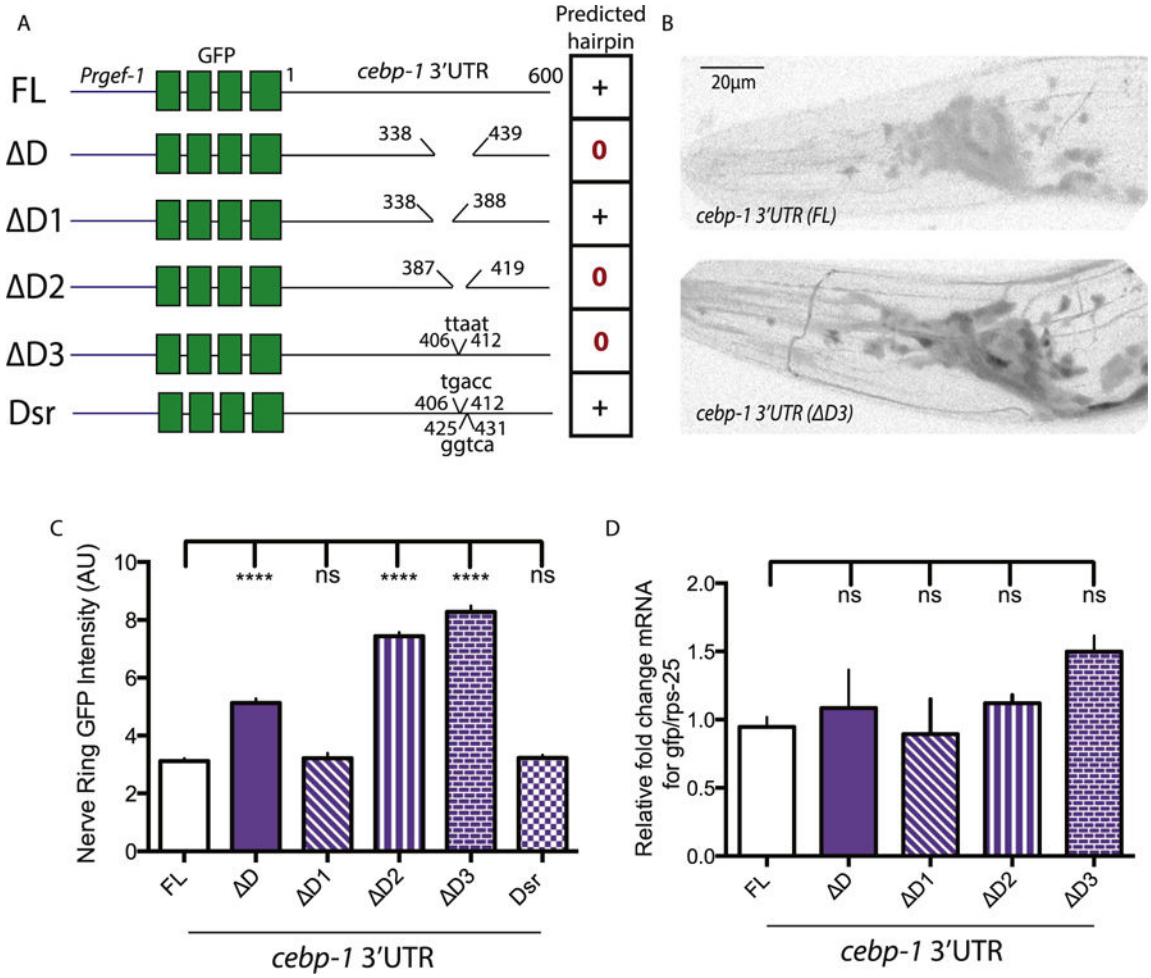

Fig. 2.

cis element D likely has a putative stem-loop secondary structure and may mediate translation of GFP reporter. A) Schematic of expression constructs for ΔD, ΔD1-3 and Dsr *cebp-1* mutant 3′ UTR reporters. Prediction for presence (+) or absence (0) for RNA secondary or hairpin structure in each 3′ UTR mutant is shown on the right column. B) Sample z-stack images of the nerve ring of *cebp-1* 3′ UTR (FL) and ΔD3 reporter in wild type background. Scale bar, 20 μm. C) Quantification of GFP in the nerve ring of L4 stage animals. n ≥ 10 for each genotype. D) qRT-PCR for GFP mRNA in L4 animals; *rps-25* used as a reference. 3 biological replicates for each strain. C-D: Error bars, SEM. Statistics, One-way ANOVA with Tukey's post hoc tests, **** $p < 0.0001$; ns, not significant.

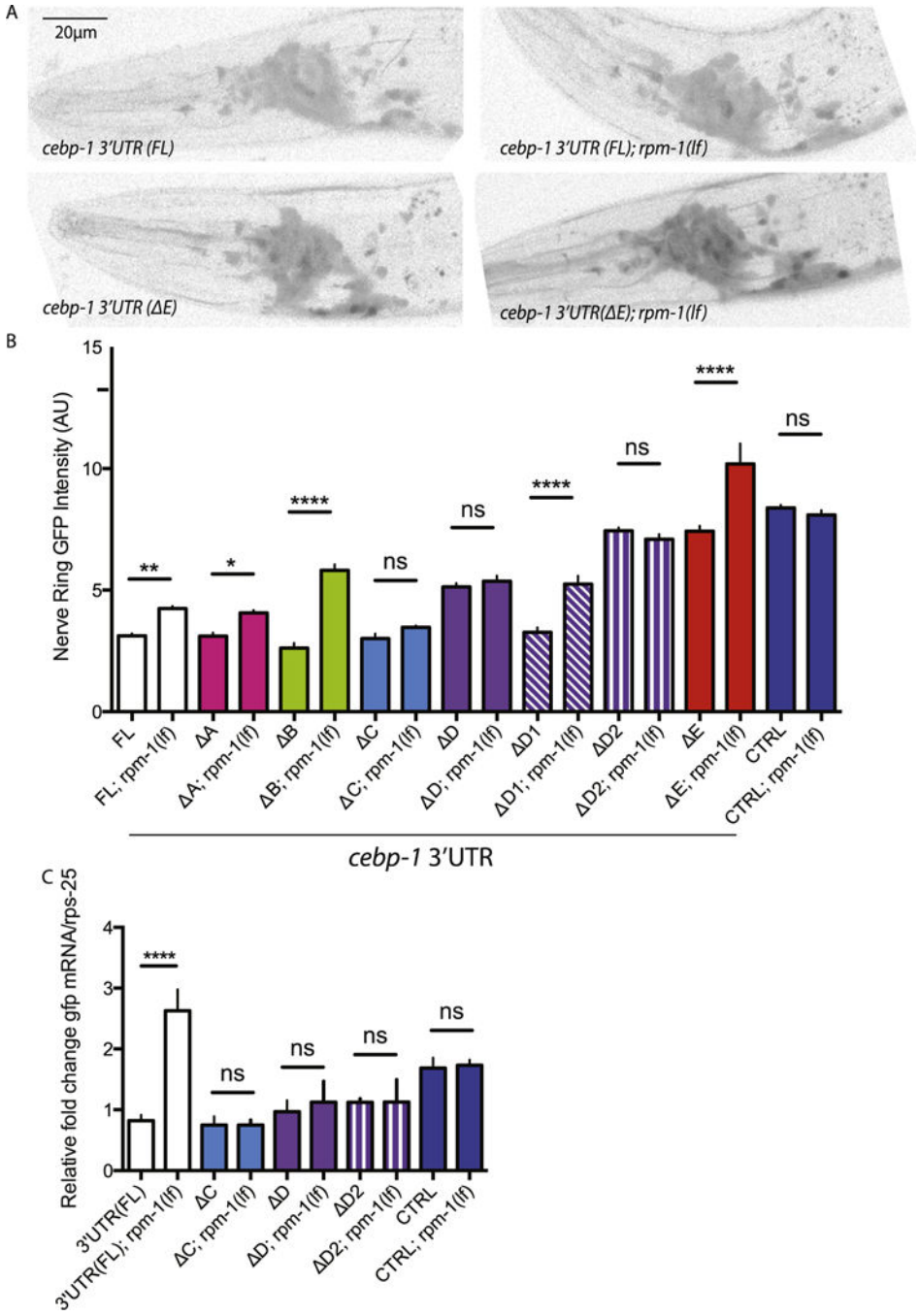

Fig. 3.

rpm-1 regulates *cebp-1* 3′ UTR reporters through *cis* elements C and D2. A) Sample z-stack images of GFP expression in nerve ring from *cebp-1* 3′ UTR (FL) and *cebp-1* 3′ UTR(ΔE) reporters in wild type and *rpm-1(lf)* background. Scale bar, 20 µm. B) Quantification of GFP in the nerve ring of L4 stage animals. Strains grown at 25 °C. n ≥ 10 for each genotype. Error bars, SEM. **** $p < 0.0001$ (One-way ANOVA with Tukey's post hoc tests). C) qRT-PCR for GFP mRNA in L4 animals; *rps-25* used as a reference gene. 3 biological replicates for each strain, except that data for *CTRL; rpm-1(lf)* were from 2 biological replicates. Error

bars, SEM. ns, not significant, *** $p < 0.001$ (One-way ANOVA with Tukey's post hoc tests).

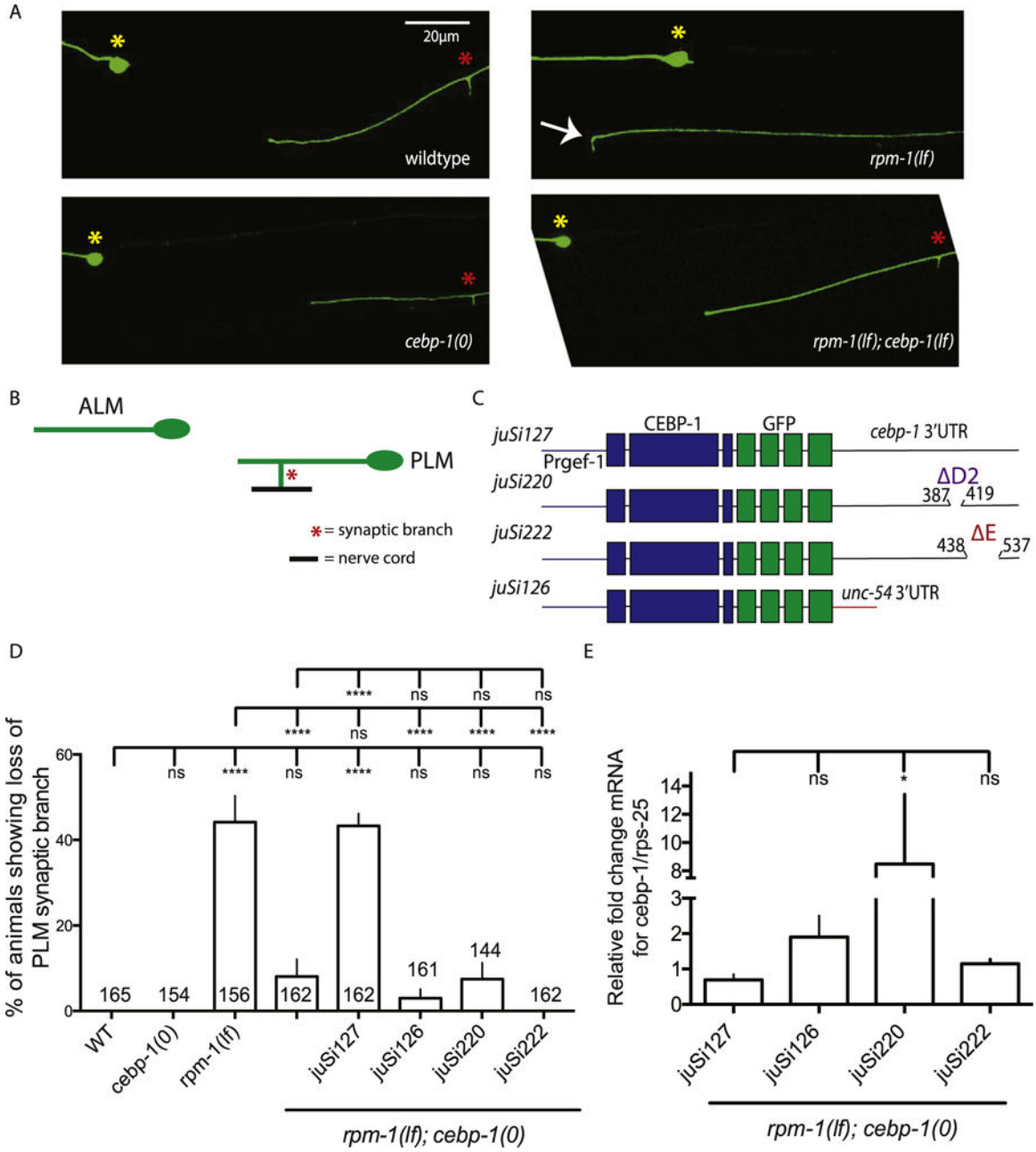

Fig. 4.

cis elements D and E in 3′ UTR are required for proper function of CEBP-1 in mechanosensory neuron development. A) Sample z-stack images of PLM neuron axon morphology in wild type, *rpm-1(lf), cebp-1(0), rpm-1(lf); cebp-1(0).* Anterior is to the left, arrow denotes the “hook” phenotype (Schaefer et al., 2000), red asterix denotes the synaptic branch from the PLM to the nerve cord, and yellow asterix denotes the ALM cell body. Scale bar, 20 μm. B) Schematic of ALM and PLM mechanosensory neuron in wild type animals. Red asterix denotes the synaptic branch from PLM to nerve cord (labeled in black) C) Schematic of pan-neural expression of CEBP-1 protein with full-length 3′ UTR or deletion of *cis* elements D2 or E. Single-copy transgene is inserted on Chromosome II. D)

Percentage of synaptic branch loss in strains expressing various MosSci transgenes of CEBP-1 in *rpm-1(lf); cebp-1(0)*. WT represents wild-type. Quantification was from 3 biological replicates, total number of animals are shown in each column. E) qRT-PCR for *cebp-1* mRNA from L4 animals of each single-copy CEBP-1 transgene in the *rpm-1(lf); cebp-1(0). rps-25* used as a reference gene for qRT-PCR. 3 biological replicates for each strain used. D-E: Error bars, SEM. ns, not significant, **** $p < 0.0001$ * $p < 0.05$ (One-way ANOVA with Dunn's multiple comparisons test).

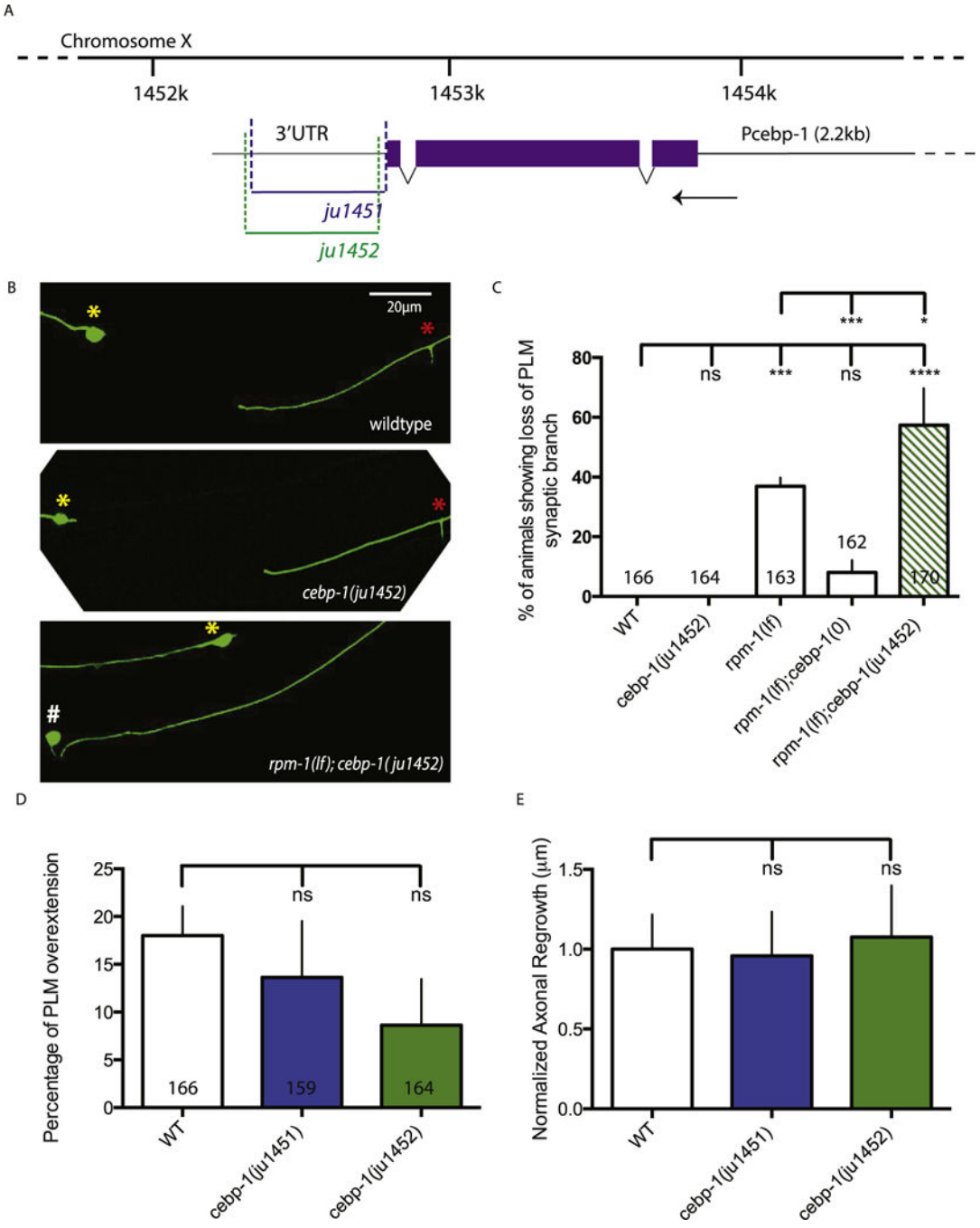

Fig. 5.

Deletion of endogenous *cebp-1* 3′ UTR results in enhanced touch neuron developmental phenotypes of *rpm-1(lf)*. A) Genome alignment of *cebp-1* with black arrow showing direction of transcription/translation. Deletions *ju1451* and *ju1452* shown in relation to *cebp-1* 3′ UTR with dotted lines. B) Sample z-stack images of PLM axon in wild type, *cebp-1(ju1452)*, and *rpm-1(lf); cebp-1(ju1452)*. Anterior is on the left, red asterix denotes the synaptic branch from the PLM to the nerve cord, yellow asterix denotes the ALM cell body, and white hashtag represents the AVM. Scale bar, 20 μm. C) Percentage of synaptic

branch loss in different strains. Experiments from 3 biological replicates with total number of animals are shown for each genotype. D) Quantification of PLM overextension in wild type, *cebp-1(ju1451)*, *cebp-1(ju1452)*. Experiments from 3 biological replicates with total number of animals are shown for each genotype. E) Normalized regrowth 24 h after axotomy in L4 worms, n > 25 worm each group. C-E: Error bars, SEM. Statistics, One-way ANOVA with Tukey's post hoc tests; ns, not significant; * $p < 0.05$, *** $p < 0.001$.

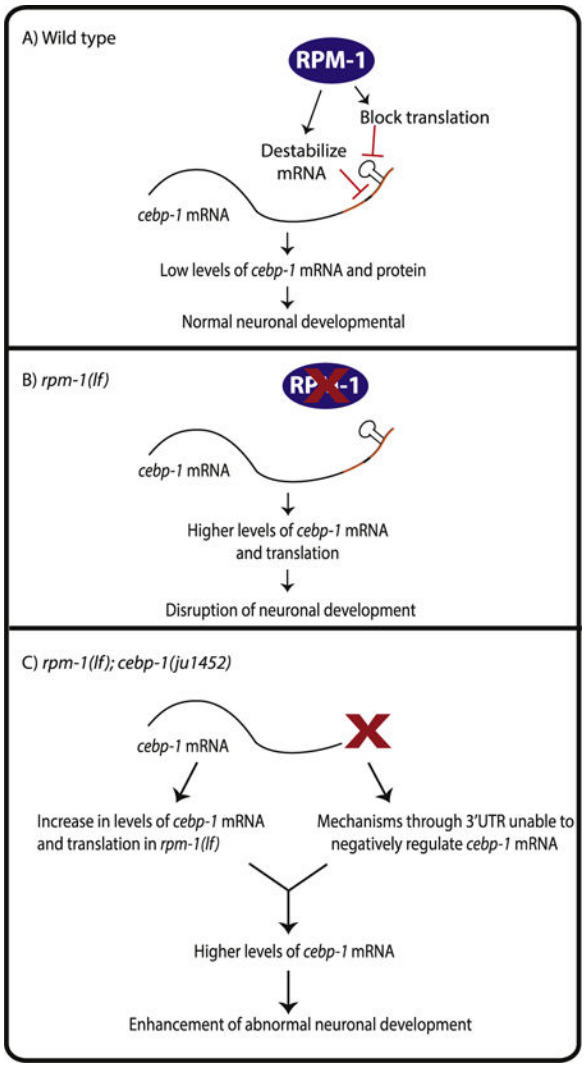

Fig. 6.

Model of *cebp-1* 3′ UTR's role. A) In wild type background or with *rpm-1* signaling, *cebp-1* levels are kept low under negative regulation by RPM-1, which partly depends on its 3′ UTR (labeled in orange) through a putative stem-loop and element C. B) In *rpm-1(lf)* background, negative regulation is absent, leading to increased *cebp-1* mRNA levels and abnormal neural development. C) *rpm-1(lf)*, in conjunction with deletion of *cebp-1*'s 3′ UTR, leads to a further increase in *cebp-1* mRNA leading to enhancement of abnormal neural development.